Iranian Journal of Basic Medical Sciences
ijbms.mums.ac.ir

Kurarinone: From chemistry to pharmacological values–A review

Huy Dinh Vu [1#], Huynh Thi Ngoc Ni [2#], Tran Thi Thanh Thuy [1], Ninh The Son [3*]

[1] Department of Chemistry, Vietnam National University of Forestry, Xuan Mai, Hanoi 10000, Vietnam
[2] Faculty of Education, Ha Tinh University, Cam Binh, Hatinh 480000, Vietnam
[3] Institute of Chemistry, Vietnam Academy of Science and Technology (VAST), 18 Hoang Quoc Viet, Nghia Do, Hanoi 10000, Vietnam

ARTICLE INFO

Article type:
Review

Article history:
Received: Nov 10, 2025
Accepted: Mar 8, 2026

Keywords:
Kurarinone
Molecular mechanism
Pharmacokinetics
Pharmacology
Phytochemistry
Sophora flavescens

ABSTRACT

Kurarinone (KRN) is a major prenylated flavanone isolated from *Sophora flavescens*, widely recognized for its diverse pharmacological activities and growing therapeutic relevance. This review provides a comprehensive and updated overview of KRN, encompassing its botanical occurrence, phytochemical characteristics, structural elucidation, and biotransformation pathways, alongside in-depth analyses of its pharmacological activities, molecular mechanisms, and pharmacokinetic behavior across experimental models. A structured literature search was conducted across PubMed, Scopus, Web of Science, and Google Scholar using the keywords "Kurarinone," "*Sophora flavescens* flavonoids," "prenylated flavanones," and related terms. Studies reporting natural occurrence, chemical isolation, biotransformation, physicochemical properties, pharmacological mechanisms, pharmacokinetics, and toxicity were included. *In vitro* and *in vivo* experimental studies and clinical disease models were prioritized, while non-primary sources and incomplete reports were excluded. KRN exhibited a broad pharmacological profile, including anticancer, anti-inflammatory, antibacterial, antiviral, and organ-protective effects, driven by its capacity to orchestrate multiple signaling networks. Mechanistically, KRN regulated pivotal molecular pathways, such as NF-κB, MAPK, JAK2/STAT3, PI3K/Akt, Nrf2/HO-1, and caspase-dependent apoptosis, thereby modulating inflammatory responses, oxidative stress, and cell apoptosis. Biotransformation studies reveal rapid conversion into glucuronide and hydroxyl conjugates. pharmacokinetic evidence indicated poor oral bioavailability (less than 50%), extensive Phase II metabolism, and tissue-specific accumulation, particularly in hepatic compartments. While these characteristics may contribute to therapeutic action, dose-dependent hepatotoxicity has been reported, highlighting critical translational challenges and the need for formulation advances and safety optimization. Future research should emphasize pharmacokinetic-pharmacodynamic modeling, nano-delivery systems, toxicity profiling, and well-designed clinical studies to support its translational development.

▶ Please cite this article as:
Vu HD, Ni HTN, Thuy TTT, Son NT. Kurarinone: From chemistry to pharmacological values–A review . Iran J Basic Med Sci 2026; 29: 675-687.
doi: https://dx.doi.org/10.22038/ijbms.2026.92633.19997

Introduction

Flavonoids are a large and structurally diverse group of phenolic compounds that represent one of the most biologically significant phytochemical classes in the plant kingdom. Structurally characterized by a C6-C3-C6 phenylchroman backbone, flavonoid derivatives encompass several subgroups, such as flavones, isoflavones, flavanones, isoflavones, pterocarpans, chalcones, and anthocyanidins. These molecules play key physiological roles in plants, including pigmentation, UV protection, and defense against pathogens. In recent decades, flavonoids have attracted increasing scientific attention due to their broad pharmacological potential, notably anticancer, anti-oxidant, antimicrobial, anti-inflammatory, hepatoprotective, and cardioprotective activities (1, 2). Their multifunctional properties, combined with relatively low toxicity and wide dietary availability, position flavonoids as promising candidates for drug discovery and therapeutic development in modern medicine.

Kurarinone (KRN) is a prenylated flavanone primarily isolated from the roots of *Sophora flavescens* Aiton (the bean family, Fabaceae), a well-known traditional medicinal plant widely utilized in East Asian medicine for treating fever, inflammation, skin disorders, and viral infections (3, 4). Chemically, the 8-prenyl group and 5-methoxy substitution distinguish its structure (molecular formula $C_{26}H_{28}O_6$)(Figure 1), which confer enhanced lipophilicity and contribute to its favorable interaction with biological membranes and signaling proteins.

Over recent years, KRN has attracted increasing scientific attention due to its broad pharmacological spectrum, including anticancer, anti-inflammatory, antibacterial, and antiviral effects, particularly its protective effects on vital organs (5-9). Mechanistic studies have demonstrated that KRN regulates multiple key molecular pathways, such as the NF-κB, MAPK, STAT3, Nrf2/HO-1, and cGAS-STING signaling pathways, thereby modulating immune activation, oxidative stress responses, cell cycle

*__Corresponding author:__ Ninh The Son. Institute of Chemistry, Vietnam Academy of Science and Technology (VAST), 18 Hoang Quoc Viet, Nghia Do, Hanoi 10000, Vietnam. Email: ntson@ich.vast.vn
# These authors contributed equally to this work

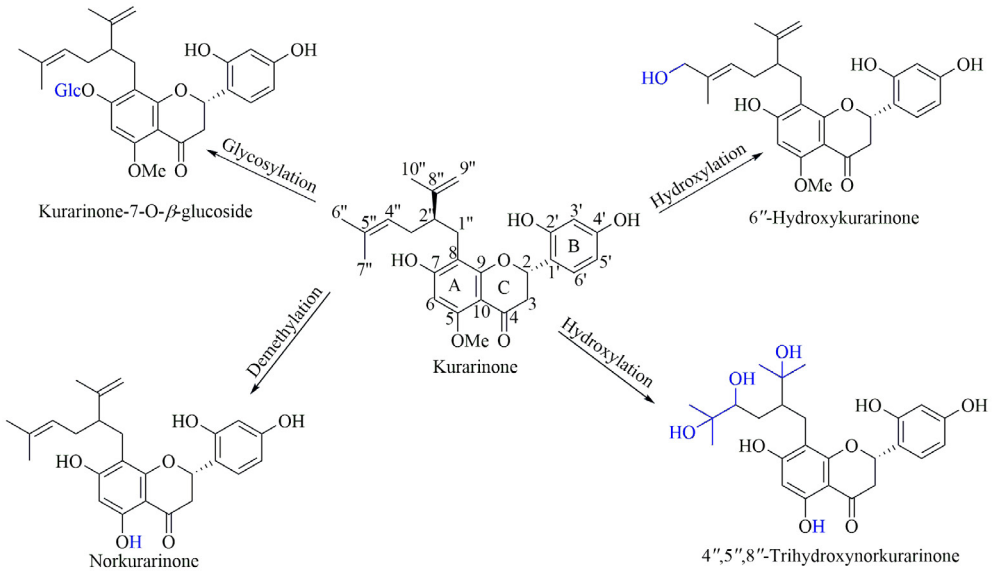

Figure 1. Chemical structure of kurarinone and its microbial biotransformation derivatives

progression, and apoptosis (10-13). In oncology research, KRN has shown the ability to induce caspase-dependent apoptosis, suppress epithelial-mesenchymal transition, and inhibit proliferative signaling, highlighting its potential as a complementary therapeutic candidate for solid tumors (14, 15). Additionally, *in vitro* and *in vivo* and pharmacological and clinical studies have reported beneficial effects of KRN in inflammatory bowel disease, metabolic dysfunction, and viral hepatitis models (16, 17).

Although numerous experimental studies have demonstrated the biological activities and therapeutic relevance of KRN across diverse disease models, comprehensive and systematically organized reviews on this compound remain limited. Existing literature primarily focuses on the isolated pharmacological findings and/or specific biological pathways, leaving a large gap in the collective understanding of its phytochemical origin, physicochemical profile, biosynthesis, and translational potential. Therefore, in this review, we comprehensively provide an integrated and updated overview of the studied flavanone KRN, encompassing its natural occurrence, physicochemical characteristics, structural elucidation, and biotransformation pathways. In addition, we critically summarize current evidence on its pharmacological activities, molecular mechanisms of action, and pharmacokinetic behavior, aiming to elucidate its therapeutic prospects and highlight key research gaps that warrant further investigation.

Natural occurrence and biotransformation

The studied flavanone was mainly found in the family Fabaceae, especially the roots of *S. flavescens*. Searching for cytotoxic agents, KRN was isolated as a single compound from the MeOH extract of Korean *S. flavescens* roots (3). The KRN content is greater in triennial *S. flavescens* than in biennial plants and is higher in lateral roots than in taproots (18). From *S. flavescens* roots, KRN was obtained with a purity of 95% using silica gel, followed by reverse-phase column chromatography (4). Under conditions of the extraction time of 30 min, methanol concentration of 80%, temperature of 80 ºC, and solvent-to-material ratio of 26 mL/g, the mean yield of KRN was 3.091 mg/g *S. flavescens* roots (19). By high-performance thin-layer chromatography (HPTLC) analysis with $CHCl_3$-MeOH (10:1, v/v) as a mobile phase, average recovery for KRN in *S. flavescens* roots was 96.3-103.4% (20). The studied compound has been promptly detectable in the alcoholic extract of *S. flavescens* roots by the hyphenated liquid chromatography-nuclear magnetic resonance (LC-NMR) technique (21).

KRN was also among the isolates from the MeOH extracts of other Fabaceae species (*S. angustifolia* roots, *S. tonkinensis* roots and rhizomes, and *Alibizzia julibrissin* stem barks), Polypodiaceae species (*Drynaria fortunei* rhizomes), Gentianaceae species (*Gentiana macrophylla* roots), and *Tetragronula* propolis (22-27).

Microbial transformation of KRN by the fungus *Cunninghamella echinulata* AS 3.3400 resulted in the production of 6”-hydroxykurarinone, 4”,5”,8”-trihydroxynorkurarinone, norkurarinone, and kurarinone-7-*O*-*β*-glucoside (28). The underlying mechanism is due to hydroxylation, glycosylation, and demethylation (Figure 1).

Physicochemical and structural elucidation

KRN was isolated as a yellow amorphous powder, and stable below 25 ˚C for 48 hr, but degradable up to 25.54% at 80 ˚C for 2 hr (4, 29). Especially, it was stable up to 21 days at -20 ˚C (30). Its optical rotation in MeOH at room temperature is +13.5, whereas the molecular ion peak has been observed at *m/z* 438 [M^+] in the electron ionization mass spectrometry (EIMS) (29). Its ^{1}H-NMR data in methanol-d_4 included the characteristic signals of the flavanone skeleton. The proton at δ_H 5.52 (1H, dd, *J*=3.0, 13.8 Hz) was assigned to H-2, confirming the presence of a saturated heterocyclic ring. The presence of two doublets at δ_H 2.84 (1H, dd, *J*=13.2, 16.8 Hz) and 2.68 (1H, dd, *J*=2.4, 16.2 Hz) corresponds to the diastereotopic protons of the methylene group at C-3, which is adjacent to the carbonyl carbon (C-4, δ_C 193.2). The signal at δ_H 6.05 (1H, br s) was attributed to H-6, consistent with a proton on an aromatic ring bearing hydroxyl substituents at C-5 and C-7 (δ_C 160.8 and 163.9, respectively). The methoxy group at δ_H 3.73 (3H,

s; δ_C 55.0) was located at C-5 according to the downfield shift of C-5 and the substitution pattern of ring A.

The B-ring exhibited an ABX spin system with δ_H 6.34 (1H, dd, J = 2.4, 8.4 Hz, H-5′), δ_H 7.28 (1H, d, J=8.4 Hz, H-6′), and δ_H 6.33 (1H, br s, H-3′), confirming a 1,3,4-trisubstituted aromatic ring. The corresponding ^{13}C-NMR signals at δ_C 158.4 (C-4′), 155.6 (C-2′), and 117.6 (C-1′) supported this substitution pattern. Additionally, resonances at δ_H 4.91 (1H, t, J=6.6 Hz, H-4″) and δ_H 4.52/4.47 (2H, d, J=1.8 Hz, H-9″) indicated the presence of a prenyl moiety, with methyl singlets at δ_H 1.41, 1.51, and 1.57 (3H each, s) corresponding to terminal isopropenyl groups. These protons correlated with carbons at δ_C 25.0, 17.0, and 18.3 ppm in the ^{13}C-NMR spectrum. The remaining carbons between δ_C 27.3-148.8 confirmed the full set of prenyl substituent signals.

Pharmacological activity

Anticancer activity

KRN showed cytotoxicity against human myeloid leukemia HL-60 and breast MCF-7/6 cancer cells with IC_{50} values of 18.5 and 22.2 μM, respectively, compared to the standard cisplatin (IC_{50} 2.3 μM)(3, 31). Treatment with KRN (10-40 μg/ml) significantly inhibited the proliferation and migration of human hepatocellular carcinoma HepG2 cells by regulating the expression of S100 calcium-binding protein A9 (S100A9) and mitogen-activated protein kinase 1 (MAPK1) through the interleukin-17 (IL-17) signaling modulation (32). At the lower doses of 0.5-1 μg/ml, KRN induced apoptosis in HepG2 cells via the reactive oxygen species (ROS) generation inhibition, as evidenced by the glutathione (GSH) depletion and mitochondrial membrane potential (MMP) disruption (33).

In another report, KRN induced p53-independent G0/G1 phase cell cycle arrest in human colorectal HCT116 cancer cells by promoting WD repeat domain 76 (WDR76)-dependent proteasomal degradation of Kirsten rat sarcoma viral oncogene homolog (K-RAS)(34). This degradation led to the suppression of the K-RAS/extracellular signal-regulated kinase (ERK)/cellular myelocytomatosis (c-MYC) signaling cascade, resulting in the down-regulation of cyclin D1/D3, cyclin-dependent kinase 4/6 (CDK4/6), and phosphorylated retinoblastoma protein (p-Rb), thereby inhibiting colorectal cancer cell proliferation (34).

KRN (40 μM) inhibited the proliferation of estrogen-unresponsive fibroblasts, ribosomal S6 kinase 2 kinase (RSK2) knockout cells, and estrogen receptor (ER)-deficient breast tumor cells, mainly by blocking phosphorylation of ERK1/2, RSK2, and S6 ribosomal protein, leading to decreased the nuclear factor-kappa B (NF-κB) transactivation and down-regulation of its target genes IL-6, cyclin D1, and superoxide dismutase 2 (SOD2)(5). In another report, KRN inhibited proliferation, induced apoptosis, and reduced cancer stem-cell-like properties in T47D, MDA-MB-231, and MCF-7 breast cancer cells through the Notch signaling suppression (35). At (1-25 μM), this molecule significantly decreased cyclin D1 expression, leading to G1-phase cell-cycle arrest, and induced mitochondria-dependent apoptosis characterized by loss of mitochondrial membrane potential and increased ROS production. KRN reduced Notch intracellular domain-dependent transcriptional activity in human embryonic kidney 293 cells and down-regulated downstream Notch target genes Hes1, Hey1, and E-cadherin (35).

KRN acted as a dual-acting anticancer agent to promote caspase-8-truncated Bid (tBid)-mitochondria crosstalk-mediated apoptosis and inhibit metastatic signaling in small-cell lung H1688 cancer cells by simultaneously activating the extrinsic and intrinsic cell-death pathways (14). Mechanistically, it increased the expression of death receptors and ligands (Fas cell surface death receptor (Fas), Fas ligand (FasL), tumor necrosis factor-related apoptosis-inducing ligand (TRAIL), death receptor 4 (DR4), and DR5), leading to caspase-8 activation (Figure 2). Activated caspase-8 cleaved caspase-3 and converted Bid into tBid, which translocated to mitochondria to trigger loss of mitochondrial membrane potential and cytochrome-c release. This mitochondrial disruption activated caspase-9, amplifying downstream caspase-3 cleavage and poly (ADP-ribose) polymerase (PARP) degradation, ultimately executing apoptosis. Concurrently, KRN down-regulated anti-apoptotic proteins Bcl-2 and Bcl-xL while up-regulating pro-apoptotic Bax, further facilitating mitochondrial permeabilization. In addition to inducing apoptosis, KRN suppressed metastatic behavior by increasing E-cadherin and reducing N-cadherin, vimentin, and MMP-2/3/9, impairing epithelial-mesenchymal transition (EMT) and limiting cancer cell migration and invasion (Figure 2).

Activating transcriptional factor 4 (ATF4) is responsible for the expression of stress-relieving and apoptosis-inducing genes (15). KRN triggered the ATF4 activation and cytostatic effects in human embryonic kidney HEK293 cells via the PKR-like endoplasmic reticulum kinase (PERK)/eukaryotic initiation factor 2 alpha (eIF2α)/ATF4 signaling pathway (15). At 20-50 μM, KRN induced PERK phosphorylation, elevated ATF4, tribbles homolog 3 (TRB3), and C/EBP homologous protein (CHOP) expression, and up-regulated the cell-cycle inhibitor p21, leading to G1 phase arrest and growth suppression. The PERK inhibition abolished these effects, confirming cytostatic action through PERK-dependent ATF4 activation (15). At the same dose, KRN protects human ovarian granulosa KGN cells from H_2O_2-

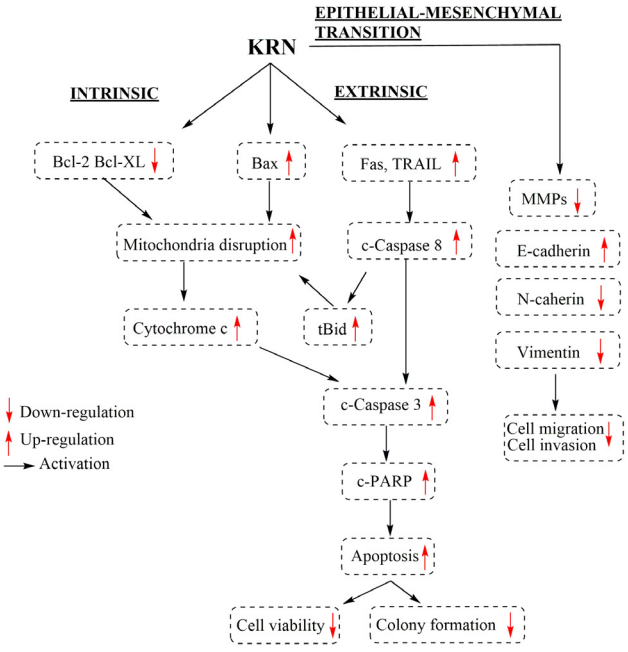

Figure 2. Anticancer mechanism of kurarinone (KRN) against the growth of small cell lung carcinoma cells

induced oxidative stress and apoptosis by activating the phosphatidylinositol 3-kinase (PI3K)/protein kinase B (Akt) signaling pathway (36). Evidently, KRN up-regulated insulin-like growth factor-1 (IGF1) expression, which in turn promoted phosphorylation of PI3K and Akt, leading to enhanced SOD1 activity, and heme oxygenase-1 (HO-1) and NAD(P)H:quinone oxidoreductase 1 mRNA expression, and suppression of ROS and malondialdehyde (MDA) levels. Silencing IGF1 abolished these protective effects (36).

KRN suppressed colon cancer stem-like cells by targeting the cluster of differentiation 44 (CD44)/janus kinase 2 (JAK2)/signal transducer and activator of transcription 3 (STAT3) axis, reducing stemness, inducing apoptosis, and causing G1-phase arrest (12). In HCT-116 monolayer cells and colonospheres, KRN significantly decreased phosphorylation of JAK2 and STAT3, reduced downstream proliferative proteins cyclin-D1 and CDK4, and down-regulated stemness markers (CD44)(Figure 3). Concurrently, KRN promoted intrinsic apoptosis by increasing Bax/Bcl-2 ratio, activating procaspase-3 cleavage and PARP fragmentation, and elevating cytochrome-c levels. These effects culminated in loss of self-renewal capacity, reduced sphere formation, and enhanced apoptosis in cancer stem-like populations (12).

KRN synergistically enhanced TRAIL-induced apoptosis in human gastric adenocarcinoma SGC-7901 cells by inhibiting STAT3 phosphorylation, leading to the down-regulation of anti-apoptotic proteins myeloid cell leukemia-1 (Mcl-1) and cellular FLICE-inhibitory protein (c-FLIP), which promotes caspase-3 activation and cell death (37).

Anti-inflammatory activity

KRN showed *in vitro* and *in vivo* anti-inflammatory activity against lipopolysaccharide (LPS)-induced sepsis damage in both macrophages and mice via the MAPK/NF-κB signaling inhibition, attenuating NLR family pyrin domain containing 3 (NLRP3) inflammasome formation, and preventing intracellular ROS accumulation (8). The compound suppressed the overproduction of inflammatory mediators nitric oxide (NO), prostaglandin E2 (PGE2), tumor necrosis factor-alpha (TNF-α), IL-6, and IL-1β, as well as alleviated oxidative stress. These effects occur through the inhibition of MAPK (ERK, JNK, and p38) and NF-κB signaling pathways, preventing inhibitor of kappa B alpha (IκBα) degradation and p65 nuclear translocation (8). KRN also blocked NLRP3 inflammasome activation by reducing ROS accumulation and disrupting the assembly of NLRP3-ASC-caspase-1 complexes. As a result, the expression of inducible nitric oxide synthase (iNOS), cyclooxygenase 2 (COX2), NLRP3, and cleaved caspase-1 was down-regulated, leading to decreased secretion of IL-1β (8).

KRN suppressed LPS-stimulated RAW 264.7 cells through activation of the Kelch-like ECH-associated protein 1 (Keap1)/nuclear factor erythroid 2-related factor 2 (Nrf2)/HO-1 signaling pathway (38). At 20-50 μM, it down-regulated Keap1 expression, leading to the stabilization and nuclear accumulation of Nrf2. Activated Nrf2 bound to anti-oxidant response elements in the promoters of target genes, and induced the expression of HO-1 and other anti-oxidant enzymes. The increased HO-1 then mediated the suppression of pro-inflammatory mediators, such as IL-1β and iNOS (38). A study in 2024 also reported that KRN at 10 mg/kg could alleviate thermal hyperalgesia and mechanical hypersensitivity in mice subjected to Complete Freund's adjuvant-induced inflammatory pain through hind paw injection (39).

Antimicrobial and antiviral activities

KRN showed the minimum inhibitory concentration (MIC) values of 6.25 μg/ml against the bee-pathogenic

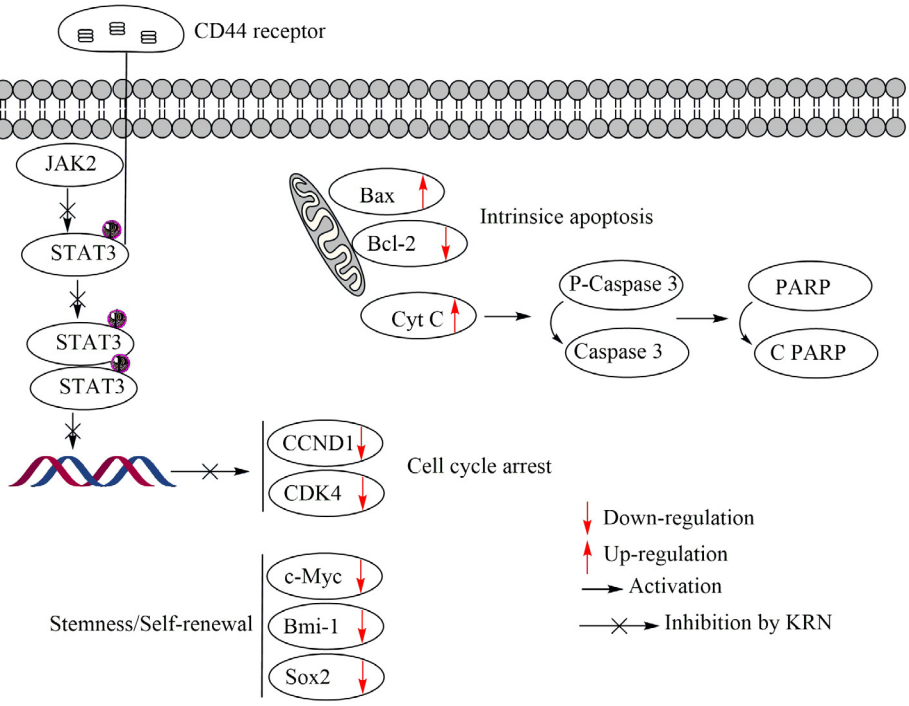

Figure 3. Anticancer mechanism of kurarinone (KRN) against the growth of colon cancer cells

bacterium *Paenibacillus larvae* KACC 14031, and 12.5 µg/ml against *P. larvae* ATCC 9545 after 48 hr, while its activity against *Melissococcus plutonius* ATCC 35311 was recorded at 12.5 µg/ml after both 24 and 48 hr. In agar diffusion tests, it produced inhibition zones of 14-16 mm at the tested concentration of 10 µg/ml (40). Checkerboard synergy analysis revealed weak to moderate synergistic interactions when combined with the standards tetracycline (fractional inhibitory concentration index (FICI)=0.88±0.10) or macelignan (FICI=0.75±0.25) (40). KRN was also found to exert MIC values of 6.25-12.5 µg/ml against the Gram-positive bacteria *Staphylococcus aureus* and *Streptococcus mutans* (Table 1)(41). KRN established the same MIC value of 2.0 µg/ml against methicillin-resistant *S. aureus* (MRSA) and vancomycin-resistant enterococci (VRE), which outperformed those of the standards ampicillin and vancomycin (42).

A study in 2024 also reported that KRN displayed potent antibacterial activity against MRSA by primarily targeting the bacterial membrane (43). The topical administration at 7.8 mg/kg significantly improved MRSA-infected wound healing and reduced bacterial load. It disrupted membrane integrity and fluidity, leading to depolarization and increased permeability, while also impairing cell-wall and biofilm biosynthesis. KRN has further interfered with bacterial energy metabolism, reducing ATP production and

Table 1. Pharmacological activities of kurarione

Models	Concentrations	Effects	References
		Anticancer activity	
In vitro		IC_{50} = 18.5 µM/HL-60 cells IC_{50} = 22.2 µM/MCF-7/6 cells	(3, 31)
In vitro	10-40 µg/ml	To inhibit the growth and migration of HepG2 cells via the IL-17 signaling pathway	(32)
In vitro	1-5 µg/ml	Apoptosis in HepG2 via the ROS generation inhibition	(33)
In vitro	10-30 µM	To induce p53-independent G0/G1 cell cycle arrest in HTC116 via the WDR76 signaling	(34)
In vitro	40 µM	To inhibit the growth of L929sA, MCF-7/6 and MDA-MB231 cells via the ERK/RSK2/NF-κB signaling pathway	(5)
In vitro	1-25 µM	Apoptosis in T47D, MDA-MB-231, and MCF-7 cells through the Notch signaling pathway	(35)
In vitro	3.125-25 µM	Apoptosis in HTC1688 cells via the mitochondria-mediated and receptor-mediated apoptotic pathways	(14)
In vitro	20-50 µM	To trigger the ATF4 activation and cytostatic effects in HEK293 cells via the PERK/eIF2α/ATF4 signaling pathway	(15)
In vitro	20-50 µM	Apoptosis in KGN cells via the PI3K/Akt signaling pathway	(36)
In vitro	1-25 µM	Apoptosis in HCT-116 cells via the CD44/JAK2/STAT3 signaling pathway	(12)
In vitro	KRN (5 µM)+TRAIL (50 ng/ml)	Apoptosis in SGC-7901 cells via the STAT3 signaling inhibition	(37)
		Anti-inflammatory activity	
In vitro	5-20 µM	To inhibit LPS-stimulated macrophages via the MAPK/NF-κB/ROS/NLRP3 signaling pathway	(8)
In vivo	20-40 mg/kg, IP	To inhibit LPS-stimulated mice via the MAPK/NF-κB/ROS/NLRP3 signaling pathway	(8)
In vitro	20-50 µM	To inhibit LPS-stimulated RAW 264.7 cells via the Keap1/Nrf2/HO-1 signaling pathway	(38)
In vivo	10 mg/kg, IP	To inhibit inflammation in the hind paw of mice	(39)
		Antimicrobial activity	
In vitro		MIC = 6.25 µg/ml/ *Paenibacillus larvae* KACC 14031/24 and 48 h MIC = 6.25 µg/ml/ *Paenibacillus larvae* ATCC 9545/24 hr MIC = 12.5 µg/ml/ *Paenibacillus larvae* ATCC 9545/48 hr MIC = 12.5 µg/ml/ *Melissococcus plutonius* ATCC 35311/24 and 48 hr	(40)
In vitro		MIC = 6.25 µg/ml/ *Streptococcus mutans* C67-1(c), *S. mutans* OMZ176(d), *S. mutans* 6715(g), *Staphylococcus aureus* HS1(a), *S. aureus* FA1(b) MIC = 12.5 µg/ml/*S. aureus* 209P, *S. mutans* Ingbritt(c), *S. mutans* OMZ175(f)	(41, 42)
In vivo	Topical	MIC = 2.0 µg/ml/MRSA and VRE improved MRSA-infected wound healing and reduced bacterial load	(43)
In vitro		EC_{50} = 16.12 µg/ml/ *Rhizoctonia solani* EC_{50} = 25.33 µg/ml/*S. sclerotiorum* EC_{50} = 16.55 µg/ml/ *Botrytis cinerea* EC_{50} = 16.99 µg/ml/ *Fusarium graminearum* EC_{50} = 22.44 µg/ml/*F. oxysporum* EC_{50} = 39.14 µg/ml/*F. verticillioide*	(44)
In vitro	10-25 µg/ml	To inhibit *B. cinerea* by affecting the cell wall and regulating cellular energy metabolism	(44)
		Antiviral activity	
In vitro		IC_{50} = 3.46 ± 0.10 µM/HCoV-OC43 coronavirus	(6)
In vitro	3-5 µM	HCoV-OC43 infectious inhibition in MRC-5 cells by impairing the virus-induced autophagic flux	(6)
		Vasorelaxant activity	
In vitro		IC_{50} = 1.1 ± 0.3 µM/Cav3.2 channels in tsA-201 cells IC_{50} = 10.4 µM/SGLT1 IC_{50} = 1.7 µM/SGLT2	(39, 45)
In vitro	1-30 µM	To potentiate the BKCa channel in AD-293 cells	(46)
In vivo	0.5-5 mg/kg, p.o.	To reduce micturition frequency in hypertensive rats	(46)
In vitro		IC_{50} = 19.2 µg/ml/THP-1-induced MCP-1 cells	(47)
In vitro	25-50 µg/ml	To inhibit the binding of MCP-1 to THP-1 cells and phosphorylation of p42/44 MAPK	(47)
In vitro	10-100 µM	To inhibit Ca^{2+} influx via a voltage-dependent Ca^{2+} channel	(7)

Continued Table 1.

		Neuroprotective activity	
In vitro		EC_{50} – 42.1 ± 0.35 μM/D_1R EC_{50} – 22.4 ± 3.46 μM/$D_{2L}R$ EC_{50} – 71.3 ± 4.94 μM/D_4R IC_{50} – 186 ± 6.17 μM/hMAO-A IC_{50} – 196 ± 12.7 μM/hMAO-B	(48)
In vitro	1-20 μg/ml	To inhibit Th1, Th2, and Th17 cell polarization and proliferation	(49)
In vivo	100 mg/kg IP	To ameliorate MOG_{35-55}-induced EAE in mice via the Th1/Th17 signaling pathway	(49)
In vitro	10-40 μM	To inhibit neuroinflammation and neurotoxicity in HMC3 cells via the IGF1/PI3K/Akt signaling pathway	(50)
In vitro	0.25-1 μM	To inhibit corticosterone-induced hippocampal neuron cells via the BACE1/PI3K/Akt signaling pathway	(51)
In vivo	50-150 mg/kg, IP	To inhibit *p*-chlorophenylalanine-induced insomnia in rats via the BACE1/PI3K/Akt signaling pathway	(51)
In vivo	10 mg/kg, IP	To suppress phase II of formalin-induced nocifensive behaviors in rats	(39)
In vivo	5-20 mg/kg, p.o.	To alleviate Parkinson's symptoms via the stabilization of epoxyeicosatrienoic acids	(52)
		Lung protective activity	
In vitro	5-10 μM	To inhibit TGF-β-induced EMT in BEAS-2B cells via the TGF-β signaling pathway	(53)
In vivo	5-10 mg/kg, p.o.	To attenuate bleomycin-induced mice via the TGF-β signaling pathway	(53)
In vitro	1-5 μM	To inhibit LPS-induced pneumonia in BEAS-2B cells via the MAPK/NF-κB signaling pathway	(13)
In vivo	100 mg/kg, p.o	To inhibit LPS-induced pneumonia in mice via the MAPK/NF-κB signaling pathway	(13)
		Renoprotective activity	
In vitro	1 μM	To alleviate high glucose-induced ferroptosis in HK-2 cells via the Nrf-2/HO-1 signaling pathway	(11)
In vitro	50 μM	To inhibit TGF-β1-induced fibrosis in HK-2 cells via the Keap1/Nrf-2 signaling pathway	(54)
In vivo	10-40 mg/kg, p.o.	To inhibit renal fibrosis and inflammation in UUO rats via the Keap1/Nrf-2 signaling pathway	(54)
		Bone protective activity	
In vitro	5-15 μM	To inhibit osteoclastogenesis in RAW264.7 and BMM cells via the MAPK signaling pathway	(55, 56)
In vivo	100 mg/kg, p.o.	To attenuate collagen-induced arthritis in mice by inhibiting Th1/Th17 cell responses and oxidative stress	(9)
In vitro	5-20 μM	To mitigate LPS-induced inflammatory osteolysis in BMM cells via the PI3K/Akt signaling pathway	(16)
In vivo	15-30 μg/g, IP	To reduce bone loss in mice via the PI3K/Akt signaling pathway	(16)
		Gastrointestinal protective activity	
In vitro	20 μg/ml	To inhibit LPS-macrophages via the AhR signaling pathway	(57)
In vivo	100 mg/kg, IP	To ameliorate intestinal inflammation in IBS mice via the AhR signaling pathway	(57)
In vitro	20 μM	To regulate Th17-like cells with pro-inflammatory regulation	(58)
In vivo	125 mg/kg, IP	To inhibit TNBS-induced colitis in mice via T cell regulation	(58)
In vitro	2-8 μM	To ameliorate ulcerative colitis by regulating Th17/Treg cell homeostasis	(59)
In vivo	20-40 mg/kg, p.o.	To inhibit DSS-induced ulcerative UC in mice via the JAK2/STAT3 signaling pathway	(59)
In vivo	20-40 mg/kg, p.o.	To inhibit DSS-induced ulcerative UC in mice via the NLRP3 signaling pathway	(60)
In vivo	5-20 μM	To inhibit ISD-induced THP-1 cells via the STING signaling pathway	(10)
In vivo	10-20 mg/kg, p.o.	To inhibit DSS-induced inflammatory bowel disease in mice via the STING signaling pathway	(10)
		Eye protective activity	
In vitro	10–20 μg/ml	To diminish AU in CDLN and PBM cells via the Rac1 inhibition	(61)
In vivo	10–40 mg/kg, IP	To diminish AU in mice via the Rac1 inhibition	(61)
		Skin protective activity	
In vitro	≤ 20 μM	To inhibit $CD4^+$ T-cell differentiation via the JAK/STAT and TCR-mediated signaling pathway	(62)
In vivo	Topical	To reduce psoriasis and dermatitis in mice via the JAK/STAT and TCR-mediated signaling pathway	(62)

elevating ROS, ultimately causing rapid cell death (43).

KRN exhibited pronounced antifungal efficacy, with EC_{50} values of 16.12, 16.55, and 16.99 μg/mL against *Rhizoctonia solani*, *Botrytis cinerea*, and *Fusarium graminearum*, respectively (44). The inhibitory mechanism against *B. cinerea* is due to the disruption of cell wall components, impairment of cell membrane integrity, increase of cell membrane permeability, and regulation of cellular energy metabolism (44). Evidently, KRN increased chitinase and β-1,3-glucanase activities while down-regulating chitin synthase-related genes (BcCSHI, BcCSHIIIa, BcCSHIIIb, BcCSHV, and BcCSHVI). It reduced ergosterol content, elevated MDA levels, and induced ROS accumulation through up-regulation of Bcrac, BcnoxA, BcnoxD, and BcnoxR (44). Additionally, it decreased ATP content, suppressed Na^+/K^+-ATPase and Ca^{2+}/Mg^{2+}-ATPase activities, and inhibited key tricarboxylic acid cycle enzymes SDH, α-KGDHC, PDH, ICDHm, NADP-MDH, and CS (44).

KRN exhibited antiviral activity against human HCoV-OC43 coronavirus with an IC_{50} of 3.46±0.10 μM and a CC_{50} value of 7.95±0.15 μM (6). Mechanistically, KRN inhibited coronavirus infection by blocking virus-induced autophagy via p62/sequestosome 1 accumulation and microtubule-associated protein 1A/1B-light chain 3 modulation, preventing replication complex formation and viral protein expression (6).

Vasorelaxant activity

KRN acted as a nonselective T-type channel antagonist that suppressed Cav3.2 channels exhibited in tsA-201 cells with an IC_{50} of 1.1±0.3 μM, and inhibited native T-type

channels in mouse dorsal root ganglion neurons (39). *In silico* study revealed that the phenyl ring, lavandulyl, and hydroxyl groups of KRN interact directly with the pore domains of all three T-type Ca channels via hydrogen and hydrophobic interactions (39). KRN showed potential Na^+-glucose cotransporter (SGLT) inhibitory activity with IC_{50} values of 10.4 μM/SGLT1 and 1.7 μM/SGLT2, compared to those of the standard phlorizin (IC_{50} 0.1-0.2 μM) (45).

KRN exhibited potent smooth-muscle-relaxant activity primarily by directly potentiating arge-conductance Ca^{2+}-activated K^+ (BKCa) channels, which stabilized the open channel conformation, shifted activation to more negative voltages, and markedly slowed deactivation of BKCa channels, leading to membrane hyperpolarization and reduced detrusor contractility (46). Evidently, KRN enhanced BKCa channel currents in AD-293 cells and oocytes in a dose-dependent manner (1-30 μM) and relaxed rat urinary bladder strips, with significant inhibition of acetylcholine-induced contraction at 100 μM. Meanwhile, KRN (0.5-5 mg/kg, p.o.) could reduce micturition frequency in spontaneously hypertensive rats without affecting normal rats, supporting a BKCa-dependent mechanism in overactive bladder modulation (46).

KRN exhibited potent anti-atherosclerotic activity against monocyte chemoattractant protein-1 (MCP-1)-induced chemotaxis of human tamm-horsfall protein-1 (THP-1) monocytes with an IC_{50} value of 19.2 μg/ml (47). Mechanistically, it markedly inhibited the phosphorylation of p42/44 MAPK (ERK1/2) in MCP-1-stimulated THP-1 cells at 25-50 μg/ml, indicating interference with the MAPK signaling cascade that mediated monocyte migration. In addition, KRN significantly blocked the binding of MCP-1 to its receptor CCR2 in a concentration-dependent fashion, thereby preventing the initial ligand-receptor interaction essential for chemotactic activation (47).

KRN inhibited Ca^{2+} influx via a voltage-dependent Ca^{2+} channel, as evidenced by suppressed KCl and norepinephrine maximum contractions in rats and KCl contractions in rabbits (7).

Neuroprotective activity

Alterations in the expression and/or activity of brain G protein-coupled receptors (GPCRs), such as dopamine receptors (D_1R, $D_{2L}R$, D_3R, and D_4R), vasopressin receptors, and serotonin receptors, are associated with various neurodegenerative diseases (48). Functional GPCR assays indicated antagonist activity of KRN at D_1R (EC_{50} 42.1±0.35 μM) and agonist activity at $D_{2L}R$ (EC_{50} 22.4±3.46 μM) and D_4R (EC_{50} 71.3±4.94 μM) (48). KRN also exhibited modest and nonspecific inhibition toward human monoamine oxidase (hMAO) isoenzymes (hMAO-A: IC_{50} 186±6.17 μM and hMAO-B: IC_{50} 196±12.7 μM)(48).

KRN exerted strong immunomodulatory effects against autoimmune neuroinflammation (49). KRN significantly ameliorated myelin oligodendrocyte glycoprotein (MOG_{35-55})-induced experimental autoimmune encephalomyelitis (EAE) in mice. The treatment markedly reduced spinal cord inflammation, demyelination, and infiltration of $CD4^+$ and $CD8^+$ T cells into the central nervous system (CNS). Moreover, KRN down-regulated mRNA expression of cytokines interferon-gamma (IFN-γ), IL-1β, IL-6, IL-17A, and TNF-α, as well as chemokines C-C motif chemokine ligand 17 (CCL17), CCL20, CCL27, and C-X-C motif chemokine ligand 1 (CXCL1)(49). It also caused a significant reduction in the percentages of T helper 1 (Th1) ($CD4^+$ IFN-γ^+) and Th17 ($CD4^+$ IL-17^+) cells in both the CNS and spleen. *In vitro*, KRN inhibited Th1, Th2, and Th17 cell polarization and proliferation. Mechanistically, KRN suppressed the expression of lineage-specific transcription factors and phosphorylation of key STAT signaling proteins: T-bet/p-STAT1/p-STAT4 in Th1 cells, GATA-3/p-STAT5/p-STAT6 in Th2 cells, and retinoic acid receptor-related orphan receptor gamma t (RORγt)/p-STAT3 in Th17 cells (49).

KRN also alleviated hemin-induced neuroinflammation and microglia-mediated neurotoxicity in human microglial HMC3 cells by promoting M2 polarization and suppressing oxidative injury via the IGF1/PI3K/Akt signaling axis (50). Herein, KRN (10-40 μM) significantly promoted anti-inflammatory M2 polarization (up-regulating Arg-1 and CD206) while suppressing pro-inflammatory M1 markers (CD32 and iNOS) and cytokines TNF-α, IL-6, and IL-1β (50). It also markedly increased IGF1 expression and activated PI3K/Akt signaling, as shown by elevated phosphorylation of PI3K and Akt. In the co-culture model, KRN-treated microglia reduced apoptosis and oxidative stress in neuron-like SH-SY5Y cells, decreasing ROS and MDA levels while enhancing anti-oxidant enzymes SOD and catalase (CAT)(50).

KRN exhibited notable *in vitro* neuroprotective effects against corticosterone-induced cytotoxicity on hippocampal neurons through the β-site amyloid precursor protein cleaving enzyme 1 (BACE1)/PI3K/Akt signaling modulation. KRN significantly improved cell viability and reduced apoptosis by down-regulating BACE1 expression, restoring the phosphorylation levels of PI3K and Akt, and BDNF expression (51). KRN also inhibited *in vivo* *p*-chlorophenylalanine-induced insomnia in rats, with the highest dose (150 mg/kg) showing comparable efficacy to Zaoren Anshen capsules (0.8 g/kg)(51). The intraperitoneal treatment of KRN (10 mg/kg) remarkably suppressed phase II of formalin-induced nocifensive behaviors in rats (39). KRN protects dopaminergic neurons and alleviates Parkinson's symptoms by inhibiting soluble epoxide hydrolase (sEH), stabilizing epoxyeicosatrienoic acids, and suppressing NF-κB-mediated neuroinflammation. Its potent activity at 5-20 mg/kg in mice and micromolar sEH inhibition *in vitro* highlight it as a promising natural therapeutic candidate for Parkinson's disease (52).

Lung protective activity

Idiopathic pulmonary fibrosis (IPF) is a chronic, progressive, and fatal interstitial lung disease of unknown cause, whereas transforming growth factor-β (TGF-β) and EMT are critically involved in the development and progression of lung fibrosis (63-65). It turns out that KRN attenuated IPF mainly by suppressing TGF-β-induced epithelial-EMT and Th17-mediated inflammation. It inhibited Smad2/3 and Akt phosphorylation, leading to reduced expression of fibrotic markers such as Col1α1, N-cadherin, and *α-smooth muscle actin (α-SMA)* in epithelial cells (53). In addition, KRN suppressed RORγt and IL-17 expression in Th17 cells, thereby decreasing collagen accumulation and fibrosis in the lungs of bleomycin-treated mice (53).

KRN demonstrated potent anti-inflammatory effects

against LPS-induced pneumonia by targeting MAPK and NF-κB signaling cascades (Figure 4)(13). The studied metabolite (100 mg/kg, p.o.) attenuated lung injury, reduced neutrophil infiltration, and markedly decreased MPO activity in mice. It also significantly lowered pulmonary levels of key pro-inflammatory cytokines, TNF-α, IL-6, and IL-1β, demonstrating a comparable anti-inflammatory efficacy to the standard dexamethasone. At the molecular level, KRN inhibited LPS-induced phosphorylation of JNK, p38, ERK, IκBα, and NF-κB p65, thereby preventing NF-κB nuclear translocation and subsequent transcription of inflammatory genes. *In vitro* treatment of KRN (1-5 μM) in LPS-stimulated bronchial epithelial BEAS-2B cells significantly down-regulated mRNA and protein expression of TNF-α, IL-6, IL-1β, COX-2, and iNOS (13). This dual inhibition of MAPK and NF-κB pathways suppresses cytokine production and inflammatory enzyme expression, ultimately mitigating airway inflammation and tissue injury.

Renoprotective activity

KRN could alleviate high glucose-induced ferroptosis in human kidney proximal tubular epithelial HK-2 cells through the activation of the Nrf-2/HO-1 signaling pathway (11). At the optimal concentration of 1 μM, KRN increased the expression of anti-oxidant enzymes HO-1, GPX4, and SLC7A11, and decreased the levels of ferroptosis-related proteins acyl-CoA synthetase long-chain family member 4 (ACSL4) and COX2 (11). This activation attenuated oxidative stress, reduced ROS production and lipid peroxidation, preserved mitochondrial membrane potential, and inhibited apoptosis. Furthermore, KRN suppressed the EMT by down-regulating vimentin and α-SMA and up-regulating E-cadherin, thereby preventing renal tubular fibrosis.

In another report, KRN could protect against renal damage and fibrosis after unilateral ureteral obstruction (UUO) via the improvement of the Keap1/Nrf-2 signaling pathway (54). In the *in vitro* model, KRN (50 μM) significantly suppressed TGF-β1-induced fibrosis in HK-2 cells. It decreased the mRNA and protein levels of α-SMA, TGF-β1, Smad3, and p-Smad3, as well as reduced oxidative stress by activating the Keap1/Nrf2/HO-1 (54). In the UUO rats, KRN administered at 10-40 mg/kg improved renal function and reduced serum BUN and creatinine levels. It attenuated renal fibrosis and inflammation by down-regulating TGF-β1/Smad3 and activating Nrf2/HO-1. KRN also induced M2 macrophage polarization (↑CD206, ↓F4/80), contributing to anti-inflammatory and antifibrotic effects (54).

Bone protective activity

At 5-15 μM, KRN could inhibit receptor activator of nuclear factor-κB ligand (RANKL)-induced osteoclastogenesis in RAW264.7 cells via the inhibition of the p38/MAPK signaling pathway (56). Herein, KRN significantly reduced the number of tartrate-resistant acid phosphatase (TRAcP)-positive osteoclasts, and down-regulated the expression of osteoclast-specific genes Acp5, cathepsin K, and Atp6v0d2. Long and partners also suggested that KRN inhibited osteoclastogenesis in RANKL-stimulated bone marrow-derived macrophage (BMM) cells by preventing the phosphorylation of MAPKs (ERK, JNK, and p38 MAPK), and delaying the IκB-α degradation, thereby suppressing NF-κB activation. This dual suppression leads to down-regulation of nuclear factor of activated T-cells cytoplasmic 1 (NFATc1) and cellular oncogene Fos (c-Fos), resulting in reduced transcription of osteoclast-specific genes (55).

KRN showed anti-arthritic effects via the simultaneous immunomodulatory and anti-oxidant pathways (9). The oral administration of 100 mg/kg significantly ameliorated joint inflammation in collagen-induced arthritis mice. Mechanistically, KRN suppressed Th1 and Th17 immune

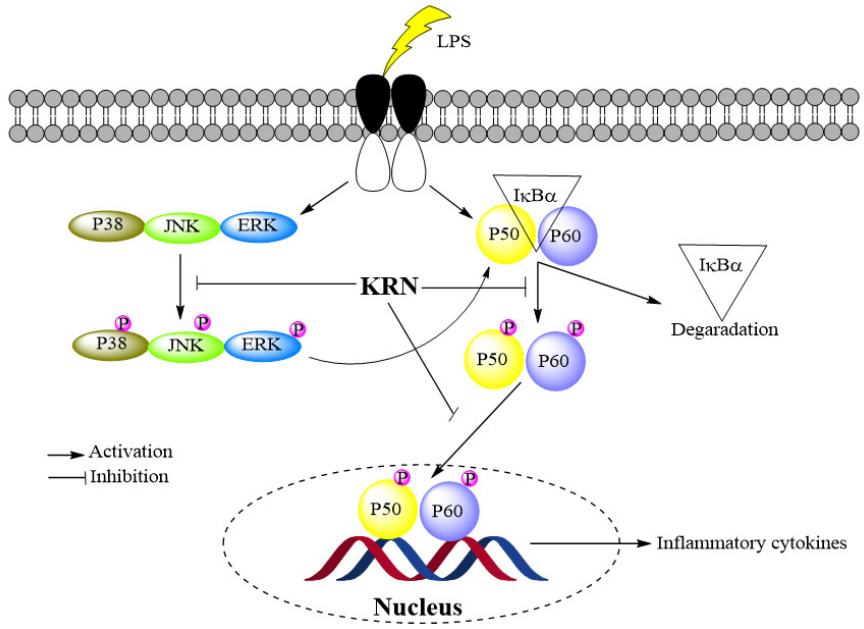

Figure 4. Mechanism of kurarinone (KRN) alleviating lipopolysaccharide (LPS)-induced pneumonia

responses by reducing T-bet and RORγt expression and inhibiting STAT1 and STAT3 phosphorylation, thereby decreasing pro-inflammatory cytokines TNF-α, IL-6, IFN-γ, and IL-17A. It also reduced CII-specific T-cell proliferation and anti-collagen IgG production, indicating inhibition of autoreactive lymphocyte activation (9). Additionally, it activated the Nrf2/HO-1 anti-oxidant pathway while down-regulating KEAP-1, resulting in increased SOD and GSH-Px activity and reduced oxidative markers such as MDA and H_2O_2 in joint tissues (9).

Inflammatory osteolysis is mainly driven by excessive osteoclast formation and oxidative stress, processes that disrupt bone remodeling and cause pathological bone resorption. As shown in Figure 5, KRN reduced inflammatory bone destruction by suppressing osteoclastogenesis through lowering ROS levels by down-regulating NADPH oxidase 1 (NOX1) and Keap1, while promoting the nuclear translocation of Nrf2 and increasing the expression of downstream anti-oxidant enzymes HO-1 and CAT (16). This dual regulation decreased oxidative stress and restored redox balance within osteoclasts. Additionally, KRN inhibited the activation of the PI3K/Akt/GSK-3β signaling pathway, thereby blocking osteoclast differentiation and bone-resorptive activity. KRN reduced the expression of osteoclast-specific markers Nfatc1, c-Fos, and Ctsk functionally. *In vivo* intraperitoneal administration of KRN significantly reduced bone loss and increased mouse anti-oxidant protein expression (16).

Gastrointestinal protective activity

KRN established potent immunoregulatory and mucosal-protective effects through macrophage-intrinsic aryl hydrocarbon receptor (AhR) activation, thereby shifting innate immune responses toward an anti-inflammatory phenotype and supporting epithelial barrier integrity (57). KRN at 20 μg/ml suppressed LPS-induced macrophage activation by down-regulating CD80, CD86, IL-1β, TNF-α, IL-12, and iNOS, while concomitantly up-regulating IL-10, Arg1, and Fizz1, resulting in reduced $CD4^+$ T-cell proliferation and IFN-γ production; importantly, these effects are abolished in AhR-deficient macrophages, highlighting an AhR-dependent mechanism (57). KRN (100 mg/kg, IP) inhibited trinitrobenzene sulfonic acid (TNBS)-induced post-inflammatory irritable bowel syndrome (IBS) in mice by alleviating visceral hypersensitivity, normalizing intestinal motility, reducing colonic pro-inflammatory cytokines, enhancing IL-10 expression, and restoring epithelial barrier function (57).

KRN demonstrated strong immunoregulatory activity in intestinal inflammation (58). For the *in vitro* model, it promoted IL-10 production and suppressed IL-17A expression in Th17-polarizing $CD4^+$ T cells by inducing the transcription factor Blimp-1, thereby generating regulatory Th17-like cells with reduced pro-inflammatory function (58). Meanwhile, the intraperitoneal administration at 125 mg/kg markedly ameliorated TNBS-induced colitis, decreasing inflammatory immune-cell infiltration, restoring goblet cells and tight-junction proteins, and increasing IL-10^+ T cells while inhibiting pathogenic Th17 responses, ultimately improving mucosal integrity and disease severity (58).

KRN exhibited potent immunomodulatory and anti-inflammatory effects against ulcerative colitis (UC)(59). The studied metabolite (2-8 μM) suppressed LPS-induced activation in RAW264.7 macrophages by reducing NO, TNF-α, and IL-6 production and preventing inflammatory morphological changes, indicating inhibition of innate immune activation. The oral administration of KRN (20-40 mg/kg) ameliorated dextran sulfate sodium salt (DSS)-induced colitis in mice, evidenced by reduced disease activity scores and improved colon histology (59). KRN restored Th17/Treg balance by decreasing IL-17A and increasing IL-10 and Foxp3, enhanced mucosal SIgA production, and inhibited JAK2/STAT3 phosphorylation, down-regulating RORγt expression and preventing aberrant Th17-mediated inflammation (59).

At the same dose of 20-40 mg/kg, KRN alleviated UC by suppressing NLRP3-inflammasome-driven intestinal

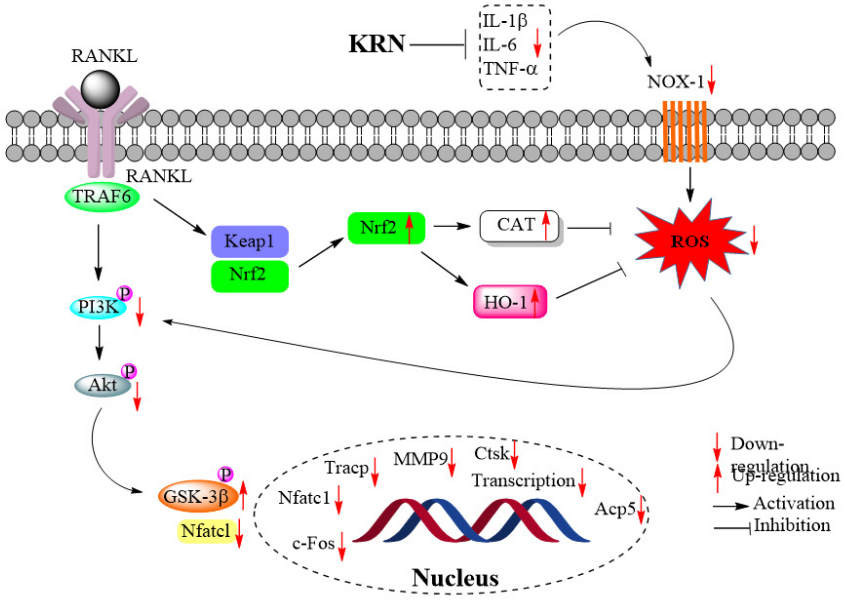

Figure 5. Inflammatory bone inhibitory mechanism of kurarinone (KRN)

inflammation and restoring macrophage homeostasis (60). It blocked NLRP3-ASC-NEK7 complex formation, preventing caspase-1 activation and IL-1β/IL-18 maturation, limiting pyroptosis and mucosal damage. KRN also reduced ROS generation and inhibited M1 polarization (iNOS, TNF-α, and IL-6 decreases), while enhancing M2 anti-inflammatory responses (IL-10 increase). By rebalancing M1/M2 macrophages within the colonic lamina propria, the studied flavonoid protected epithelial integrity, reduced disease activity, and improved histopathology in DSS-induced UC models (60).

KRN suppressed the cyclic GMP-AMP synthase (cGAS)/stimulator of interferon genes (STING) signaling pathway (10). KRN (5-20 μM) inhibited *in vitro* interferon-stimulatory DNA (ISD)-induced the activation of human monocytic leukemia THP-1 cells, markedly reducing phosphorylation of STING and interferon regulatory factor-3 (IRF3), preventing IRF3 nuclear translocation, and attenuating transcription and secretion of IFN-β, IL-6, TNF-α, IL-1β, CXCL10, and ISG15 (10). The oral administration of KRN (10-20 mg/kg) ameliorated *in vivo* DSS-induced inflammatory bowel disease, improving histopathological damage, restoring goblet cell number and mucus barrier integrity, and reducing serum IFN-β, IL-6, TNF-α, and IL-1β (10).

Eye protective activity

Autoimmune uveitis (AU) is a chronic inflammatory disorder of the eye caused by dysregulated immune responses against retinal antigens (66). The disease is mainly mediated by autoreactive $CD4^+$T cells, particularly Th17 and Th1 subsets, leading to infiltration of inflammatory cells, retinal damage, and vision impairment (61). Restoring immune tolerance and suppressing Th17-driven inflammation are therefore key strategies for controlling AU.

KRN exerted its therapeutic effect against AU by targeting the Rac1-Id2/Pim1 signaling pathway, which regulated Th17 differentiation and inflammatory responses (61). KNR inhibited Rac1 activation, leading to the down-regulation of Id2 and Pim1, thereby suppressing Th17 pathogenicity and restoring the Th17/Treg balance. *In vitro* evidence showed that KRN (10-20 μg/ml) in cervical draining lymph node (CDLN) and human peripheral blood mononuclear cells (PBM) cells markedly reduced Rac1, Id2, and Pim1 expression, as well as the production of IL-17, GM-CSF, and TNF-α. *In vivo* intraperitoneal administration at 10-40 mg/kg/day (optimal at 20 mg/kg) significantly attenuated ocular inflammation, decreased Th17/Th1 populations, and enhanced $Foxp3^+$ Tregs in mice (61).

Skin protective activity

KRN (≤20 μM) inhibited $CD4^+$ T-cell differentiation by down-regulating GATA binding protein 3 and RORγt and reducing Th2/Th17 cytokines IL-4, IL-17A, and IL-22, while increasing IL-10 and TGF-β. It suppressed cytokine-induced phosphorylation of STAT1, STAT3, STAT4, STAT5, and STAT6. It inhibited T cell receptor (TCR)-mediated Src, p38 MAPK, and Akt activation, indicating blockade of both JAK/STAT and TCR pathways (62). Topical application of KRN alleviated IL-23-induced psoriasis-like and 2,4,6-trinitrochlorobenzene-induced contact dermatitis in mice, reducing ear swelling and mRNA levels of IL-1β, IL-6, TNF-α, COX-2, and Th17 cytokines, while elevating IL-10 (62). These results show that KRN effectively suppresses inflammatory signaling and immune-mediated skin inflammation.

Clinical trials

KRN (400 mg/day, i.m.) demonstrated antiviral and immunomodulatory activity in patients with chronic hepatitis B (17) with no side effects. In this randomized trial, white blood cell and platelet counts were increased, and hepatitis B e antigen (HBeAg) and hepatitis B virus DNA clearance, with alanine aminotransferase normalization, were comparable to INF-α. Mechanistically, KRN inhibited hepatitis B surface antigen (HBsAg) and HBeAg expression, prevented hepatocyte apoptosis, and reduced liver fibrosis (17).

In the same manner, KRN, when combined with lamivudine, improved immune function in patients with chronic hepatitis B by modulating T-cell responses and the Th1/Th2 cytokine balance (67). In a 48-week trial, patients receiving this drug formula showed increased $CD4^+$ T-cell percentage, decreased $CD8^+$ T-cell percentage, and a higher $CD4^+/CD8^+$ ratio, indicating enhanced cellular immunity. Cytokine analysis demonstrated elevated IL-2 and IFN-γ, alongside reduced IL-6 and IL-10, suggesting a shift toward a Th1-dominant antiviral response (67).

Pharmacokinetics and metabolism

Pharmacokinetic parameters after intravenous administration of KRN (10 mg/kg) to rats included $T_{1/2}$ (elimination half-life) of 1.81±1.29 hr, C_{max} (peak plasma concentration) of 1668.01±101.04 ng/ml, AUC_{0-t} (area under the curve from zero to time t) of 1539.14 ± 91.07 ng.h/mL, $AUC_{0-\infty}$ (area under the curve from zero to infinity) of 1595.30±102.38 ng.h/ml, and CL (clearance) of 6.31±0.55 L.kg/hr (30). KRN demonstrated a rapid pharmacokinetic disposition in metabolic dysfunction-associated fatty liver disease (MAFLD) rats, characterized by a short elimination half-life following both intravenous ($T_{1/2}$=2.21±0.518 hr) and oral administration ($T_{1/2}$ =2.923±0.083 hr)(68). The compound exhibited rapid systemic CL with the plasma concentrations declining below quantifiable levels within 4 hr. Although oral absorption occurred efficiently, the peak plasma concentration (C_{max}=105.82±73.117 ng/ml) and AUC values (AUC_{0-t}=182.472±93.885 h.ng/ml and $AUC_{0-\infty}$ =186.46±96.841 h.ng/ml) were significantly lower than those observed after intravenous administration (68).

By intravenous administration, KRN was found to be rapidly eliminated in dog plasma, with an $T_{1/2}$ of 2.38±0.68 hr and a CL of 3.65±2.25 L/kg/hr, accompanied by a short MRT of 3.44±0.71 hr (69). Following oral dosing, the compound exhibited a notably longer $T_{1/2}$ of 4.56±1.64 hr and MRT of 9.29±1.61 hr, indicating slower elimination and sustained systemic exposure. KRN reached a C_{max} of 90.23±28.31 ng/ml at T_{max} of 4.18±0.36 hr, suggesting gradual gastrointestinal absorption. Oral administration generated markedly higher systemic exposure ($AUC_{0-\infty}$ =2926.32±603.27 ng.h/ml), compared with intravenous delivery ($AUC_{0-\infty}$=754.94±157.52 ng.h/ml)(69).

After intravenous dosing of *S. flavescens* extract, KRN exhibited a relatively short $T_{1/2}$ of 2.37±0.64 hr and rapid systemic clearance, reflected by a mean residence time (MRT=2.44±0.38 h). The C_{max} and $AUC_{0-\infty}$ reached 84.77±28.84 ng/ml and 126.70±44.92 ng.h/ml, respectively

(70). Following oral administration, KRN showed slower absorption, with T_{max} (time to peak concentration) of 4.53±2.29 hr and a similar C_{max} of 80.86±14.84 ng/ml). However, oral systemic exposure remained moderate ($AUC_{0-\infty}$=461.98±136.56 ng.h/ml), indicating poor absorption and/or extensive first-pass metabolism. The $T_{1/2}$ increased to 3.83±1.80 hr, and MRT extended to 7.91±2.13 hr, suggesting prolonged systemic retention possibly due to enterohepatic recirculation or delayed intestinal absorption (70).

The oral bioavailability of KRN in the plasma of dogs, normal rats, and MAFLD rats was about 38.19, 50.27, and 17%, respectively (68-70). In rat urine and human liver microsomes, KRN has been transformed into non-toxic metabolites with hydroxylation (minor, ≤1.4%) and or glucornidation (major, 28.7-30.2%) of its hydroxyl groups via the catalysis by phase II metabolism enzymes, such as glucuronosyltransferases (UGTs: UGT1A3, UGT1A9, and UGT1A1, UGT2B4, and UGT2B7) (71, 72). KRN, the major flavonoid of *S. flavescens*, was also metabolized by CYP1A2 and CYP2D6 and strongly inhibited UGT1A6, CYP1A2, and CYP2C9 (>90% inhibition at 100 μM)(73). KRN showed moderate permeability at pH 4.0 and 7.4, and high hepatic clearance, indicating oral absorption but rapid metabolism, which may substantially affect co-administered drugs (73).

The oral administration of *S. flavenscens* root 70% EtOH extract resulted in the highest distribution of KRN to the liver ($AUC_{0-4\,h}$: 45.5 h.nmol/ml) and intestine (21.4 h.nmol/mL), whereas it was slightly found in the portal plasama, body plasma, kidney, heart, skeletal muscle, and biliary secretion (0.8–6.9 h.nmol/ml)(74). In MAFLD rats, KRN (50 and 100 mg/kg) prevented excessive body-weight gain and significantly reduced liver index relative to the model group, reflecting attenuation of hepatic enlargement and steatosis-associated pathology (68). Importantly, it did not significantly alter heart, kidney, spleen, or lung indices (68).

Conclusion and perspective

KRN, a lavandulylated flavanone predominantly isolated from the root extracts of *S. flavescens*, continues to attract significant scientific attention due to its structurally 8-prenyl moiety and diverse pharmacological spectrum. Extensive phytochemical investigations have enabled its isolation and structural authentication via chromatographic and spectral techniques. Accumulating evidence has highlighted its broad pharmacological spectrum, notably its anticancer, anti-inflammatory, antibacterial, and antiviral activities, especially organ protective actions. Mechanistic studies have demonstrated that KRN modulates diverse molecular pathways, such as JAK2/STAT3, NF-κB, PI3K/Akt, MAPK, and apoptotic cascades, thereby regulating cellular proliferation, inflammation, and oxidative stress. In addition, emerging pharmacokinetic data revealed rapid metabolism to the main phase-II metabolites type glucuronidation and tissue-dependent distribution, underscoring the importance of metabolic fate in shaping its bioactivity.

Despite compelling preclinical evidence and initial hepatitis clinical results, translation of KRN into clinical application remains limited by gaps in standardization, bioavailability constraints, insufficient long-term safety data, and a few of human studies. KRN-induced hepatotoxicity has been reported to be dose-dependent and is mainly attributed to its high lipophilicity and preferential hepatic accumulation, together with extensive phase II metabolism. Excessive hepatic exposure may trigger oxidative stress and mitochondrial dysfunction, highlighting hepatotoxicity as a critical safety concern for prenylated flavonoids. Formulation advances, such as nano- or lipid-based delivery systems, may improve solubility and modulate tissue distribution, thereby reducing excessive first-pass hepatic exposure and mitigating dose-dependent liver toxicity, which may facilitate safer translational development. Future research should focus on: (i) comprehensive toxicokinetic and metabolism-guided safety profiling; (ii) advanced delivery platforms such as nano-formulations, lipid carriers, and prodrug systems to enhance solubility and systemic exposure; (iii) metabolite-activity mapping to delineate the role of conjugates in therapeutic responses; and (iv) pharmacokinetics-pharmacodynamics integrated modeling to guide rational dosage design. Interdisciplinary collaboration integrating natural product chemistry, metabolomics, molecular pharmacology, and formulation science will be essential to unlock KRN's translational potential and validate its role as a promising drug-development lead.

Acknowledgment

Not applicable.

Authors' Contributions

HD V conceived the study, HTN N provided formal analysis; TTT T contributed to methodology; NT S helped supervise, review, and edit.

Conflicts of Interest

Authors declare no conflicts of interest.

Declaration

We have not used any AI tools or technologies to prepare this manuscript.

References

1. Wang ZL, Wang S, Kuang Y, Hu ZM, Qiao X, Ye M. A comprehensive review on phytochemistry, pharmacology, and flavonoid biosynthesis of *Scutellaria baicalensis*. Pharm Biol 2018; 56: 465-484.
2. Janabi AHM, Kamboh AA, Saeed M, Xiaoyu L, Bibi L, Majeed F, *et al.* Flavonoid-rich foods (FRF): A promising nutraceutical approach against lifespan-shortening diseases. Iran J Basic Med Sci 2020; 23: 140-153.
3. Kang T-H, Jeong S-J, Ko W-G, Kim N-Y, Lee B-H, Inagaki M, *et al.* Cytotoxic lavandulyl flavanones from *Sophora flavescens*. J Nat Prod 2000; 63: 680-681.
4. Liu P, Deng T, Ye C, Qin Z, Hou X, Wang J. Identification of kurarinone by LC/MS and investigation of its thermal stability. J Chil Chem Soc 2009; 54: 80-82.
5. Berghe WV, De Naeyer A, Dijsselbloem N, David J-P, De Keukeleire D, Haegeman G. Attenuation of ERK/RSK2-driven NFκB gene expression and cancer cell proliferation by kurarinone, a lavandulyl flavanone isolated from *Sophora flavescens* Ait. roots. Endocr Metab Immune Disord Drug Targets 2011; 11: 247-261
6. Min JS, Kim DE, Jin YH, Kwon S. Kurarinone inhibits HCoV-OC43 infection by impairing the virus-induced autophagic flux in MRC-5 human lung cells. J Clin Med 2020; 9: 2230.
7. Yamahara J, Kobayashi G, Iwamoto M, Chisaka T, Fujimura H, Takaishi Y, *et al.* Vasodilatory active principles of *Sophora flavescens* root. J Ethnopharmacol 1990; 29: 79-85.
8. Yazal T, Lee PY, Chen PR, Chen IC, Liu PL, Chen YR, *et al.* Kurarinone exerts anti-inflammatory effect via reducing ROS

production, suppressing NLRP3 inflammasome, and protecting against LPS-induced sepsis. Biomed Pharmacother 2023; 167: 115619.
9. Tang KT, Lin CC, Lin SC, Wang JH, Tsai SW. Kurarinone attenuates collagen-induced arthritis in mice by inhibiting Th1/Th17 cell responses and oxidative stress. Int J Mol Sci 2021; 22: 4002.
10. Liu L, Wang Z, Qi Y, Huang A, He C, Zhan X, *et al.* Kurarinone alleviates cGAS-STING-triggered inflammatory diseases by targeting STING. Phytother Res 2025; 39: 3450-3465.
11. Ma C. Kurarinone activates the Nrf-2/HO-1 signaling pathway and alleviates high glucose-induced ferroptosis in HK2 cells. J Clin Biochem Nutr 2025; 77: 30-36.
12. Prajapati KS, Kumar S. Kurarinone targets JAK2-STAT3 signaling in colon cancer-stem-like cells. Cell Biochem Funct 2024; 42: e3959.
13. Wang L, Lu G, Wang F, Tao Y, Dai C. Kurarinone attenuates LPS-Induced pneumonia by inhibiting MAPK and NF-kappaB signaling pathways. APMIS 2025; 133: e70013.
14. Chung TW, Lin CC, Lin SC, Chan HL, Yang CC. Antitumor effect of kurarinone and underlying mechanism in small cell lung carcinoma cells. Onco Targets Ther 2019; 12: 6119-6131.
15. Nishikawa S, Itoh Y, Tokugawa M, Inoue Y, Nakashima KI, Hori Y, *et al.* Kurarinone from *Sophora flavescens* roots triggers ATF4 activation and cytostatic effects through PERK phosphorylation. Molecules 2019; 24: 3110.
16. Hao L, Luo H, Tan W, Zhong J, Xiong J, Liu Z, *et al.* Kurarinone mitigates LPS-induced inflammatory osteolysis by inhibiting osteoclastogenesis through the reduction of ROS levels and suppression of the PI3K/AKT signaling pathway. Inflammation 2025; 48: 29856-3005.
17. Chen C, Guo SM, Liu B. A randomized controlled trial of kurorinone versus interferon-alpha2a treatment in patients with chronic hepatitis B. J Viral Hepat 2000; 7: 225-229.
18. Lei H, Niu T, Song H, Bai B, Han P, Wang Z, *et al.* Comparative transcriptome profiling reveals differentially expressed genes involved in flavonoid biosynthesis between biennial and triennial *Sophora flavescens*. Ind Crop Prod 2021; 161: 113217.
19. Zhou J, Zhang L, Li Q, Jin W, Chen W, Han J, *et al.* Simultaneous optimization for ultrasound-assisted extraction and antioxidant activity of flavonoids from *Sophora flavescens* using response surface methodology. Molecules 2018; 24: 112.
20. Olennikov D. Densitometric HPTLC analysis of kurarinone and sophoraflavanone G in *Sophora flavescens* root. J Planar Chromat 2011; 24: 121-124.
21. Kim JS, Sang MK, Min CK, Suk WK, Byung HU. Fast identification of flavonoids in the roots of *Sophora flavescens* by on-flow LC-NMR. J Med Plants Res 2010; 4: 2452-2459.
22. Hatayama K, Komatsu M. Studies on the constituents of *Sophora* species. V. Constituents of the root of *Sophora angustifolia* SIEB. et ZUCC. (2). Chem Pharm Bull 1971; 19: 2126-2131.
23. Tan RX, Wolfender JL, Zhang LX, Ma WG, Fuzzati N, Marston A, *et al.* Acyl secoiridoids and antifungal constituents from *Gentiana macrophylla*. Phytochemistry 1996; 42: 1305-1313.
24. Jung MJ, Kang SS, Jung HA, Kim GJ, Choi JS. Isolation of flavonoids and a cerebroside from the stem bark of *Albizzia julibrissin*. Arch Pharm Res 2004; 27: 593-599.
25. Xinhluan W, Zhen L, Zhang G, Wong MS, Qin L, Yao X. Osteogenic effects of flavonoid aglycones from an osteoprotective fraction of *Drynaria fortunei*-an *in vitro* efficacy study. Phytomedicine 2011; 18: 868-872.
26. Ming CH, Cheng ZH, Chen DF. Qualitative and quantitative analysis of flavonoids in *Sophora tonkinensis* by LC/MS and HPLC. Chin J Nat Med 2013; 11: 690-698.
27. Sahlan M, Devina A, Pratami DK, Situmorang H, Farida S, Munim A, *et al.* Anti-inflammatory activity of *Tetragronula* species from Indonesia. Saudi J Biol Sci 2019; 26: 1531-1538.
28. Shi YQ, Xin XL, Yuan QP, Wang CY, Zhang BJ, Hou J, *et al.* Microbial biotransformation of kurarinone by *Cunninghamella echinulata* AS 3.3400. J Asian Nat Prod Res 2012; 14: 1002-1007.
29. Quang TH, Nhiem NX, Anh HLT, Tai BH, Van Minh C, Kim YH, *et al.* Flavonoids from the roots of *Sophora flavescens*. Vietnam J Chem 2015; 53: 77-81.
30. Zhang WM, Li RF, Qiu JF, Zhang ZY, Wang HB, Bian L, *et al.* Determination of kurarinone in rat plasma by UPLC-MS/MS. J Chromatogr B Analyt Technol Biomed Life Sci 2015; 986-987: 31-34.
31. Naeyer AD, Vanden Berghe W, Pocock V, Milligan S, Haegeman G, De Keukeleire D. Estrogenic and anticarcinogenic properties of kurarinone, a lavandulyl flavanone from the roots of Sophora flavescens. J Nat Prod 2004; 67: 1829-1832.
32. Jiang P, Liang Y, Cui X, Zhang Y, Peng C, Wang Q. Mechanistic research on the anti-hepatocellular carcinoma effect of kurarinone based on network pharmacology and experimental validation. Eur J Integr Med 2023; 62: 102280.
33. Kim SC, Lee JR, Park SJ. Cytoprotective effects of kurarinone against tert-butyl hydroperoxide-induced hepatotoxicity in HepG2 Cells. Herb Formula Sci 2018; 26: 251-259.
34. Kwon M, Oh T, Jang M, Kim GH, Kim JH, Ryu HW, *et al.* Kurarinone induced p53-independent G0/G1 cell cycle arrest by degradation of K-RAS via WDR76 in human colorectal cancer cells. Eur J Pharmacol 2022; 923: 174938.
35. Kushwaha PP, Shuaib M, Prajapati KS, Singh AK, Kulharia M, Kumar S, *et al.* Kurarinone, a natural notch signaling inhibitor and modulator of breast cancer stemness. Cancer Res 2023; 83: 4955-4955.
36. Li W, Yin X, Yan Y, Liu C, Li G. Kurarinone attenuates hydrogen peroxide-induced oxidative stress and apoptosis through activating the PI3K/Akt signaling by upregulating IGF1 expression in human ovarian granulosa cells. Environ Toxicol 2023; 38: 28-38.
37. Zhou W, Cao A, Wang L, Wu D. Kurarinone synergizes TRAIL-induced apoptosis in gastric cancer cells. Cell Biochem Biophys 2015; 72: 241-249.
38. Nishikawa S, Inoue Y, Hori Y, Miyajima C, Morishita D, Ohoka N, *et al.* Anti-inflammatory activity of kurarinone involves induction of HO-1 via the KEAP1/Nrf2 pathway. Antioxidants (Basel) 2020; 9: 842.
39. Ali MY, Choi JS, Huang S, Antunes FTT, Jung HA, Zamponi GW. Kurarinone, a lavandulyl flavanone from *Sophora flavescens*, inhibits t-type calcium channels and exerts analgesic effects in a mouse model of inflammatory pain. ACS Food Sci Technol 2024; 4: 2355-2364.
40. Park S, Kim J, Shin Y-K, Kim K-Y. Antimicrobial activity of 4-hydroxyderricin, sophoraflavanone G, acetylshikonin, and kurarinone against the bee pathogenic bacteria *Paenibacillus larvae* and *Melissococcus plutonius*. J Apic Res 2020; 60: 118-122.
41. Yamaki M, Kashihara M, Takagi S. Activity of Ku Shen compounds against *Staphylococcus aureus* and *Streptococcus mutans*. Phytother Res 1990; 4: 235-236.
42. Chen L, Cheng X, Shi W, Lu Q, Go VL, Heber D, *et al.* Inhibition of growth of Streptococcus mutans, methicillin-resistant *Staphylococcus aureus*, and vancomycin-resistant enterococci by kurarinone, a bioactive flavonoid isolated from *Sophora flavescens*. J Clin Microbiol 2005; 43: 3574-3575.
43. Weng Z, Zeng F, Wang M, Guo S, Tang Z, Itagaki K, *et al.* Antimicrobial activities of lavandulylated flavonoids in *Sophora flavences* against methicillin-resistant *Staphylococcus aureus* via membrane disruption. J Adv Res 2024; 57: 197-212.
44. An JX, Wang R, Li AP, Zhang W, Nan Z, Jiang WQ, *et al.* Prenylated Flavonoids isolated from the root of *Sophora flavescens* as potent antifungal agents against *Botrytis cinerea*. J Agric Food Chem 2024; 72: 19618-19628.
45. Sato S, Takeo J, Aoyama C, Kawahara H. Na+-glucose cotransporter (SGLT) inhibitory flavonoids from the roots of *Sophora flavescens*. Bioorg Med Chem 2007; 15: 3445-3449.
46. Lee S, Chae MR, Lee BC, Kim YC, Choi JS, Lee SW, *et al.* Urinary bladder-relaxant effect of kurarinone depending on potentiation of large-conductance Ca^{2+}-activated K^+ channels. Mol Pharmacol 2016; 90: 140-150.
47. Lee SW, Lee HS, Nam JY, Kwon OE, Baek JA, Chang JS, *et al.*

Kurarinone isolated from *Sophora flavescens* Ait inhibited MCP-1-induced chemotaxis. J Ethnopharmacol 2005; 97: 515-519.
48. Prajapati R, Seong SH, Paudel P, Park SE, Jung HA, Choi JS. *In vitro* and *in silico* characterization of kurarinone as a dopamine D(1A) receptor antagonist and D(2L) and D(4) receptor agonist. ACS Omega 2021; 6: 33443-33453.
49. Xie L, Gong W, Chen J, Xie HW, Wang M, Yin XP, *et al.* The flavonoid kurarinone inhibits clinical progression of EAE through inhibiting Th1 and Th17 cell differentiation and proliferation. Int Immunopharmacol 2018; 62: 227-236.
50. Jia ZQ, Zuo C, Yue WF. Kurarinone alleviates hemin-induced neuroinflammation and microglia-mediated neurotoxicity by shifting microglial M1/M2 polarization via regulating the IGF1/PI3K/Akt signaling. Kaohsiung J Med Sci 2022; 38: 1213-1223.
51. Wu G, Wu Y. Neuroprotective effect of Kurarinone against corticosterone-induced cytotoxicity on rat hippocampal neurons by targeting BACE1 to activate P13K-AKT signaling - A potential treatment in insomnia disorder. Pharmacol Res Perspect 2023; 11: e01132.
52. Sun CP, Zhou JJ, Yu ZL, Huo XK, Zhang J, Morisseau C, *et al.* Kurarinone alleviated Parkinson's disease via stabilization of epoxyeicosatrienoic acids in animal model. Proc Natl Acad Sci U S A 2022; 119: e2118818119.
53. Park SJ, Kim TH, Lee K, Kang MA, Jang HJ, Ryu HW, *et al.* Kurarinone attenuates BLM-induced pulmonary fibrosis via inhibiting TGF-beta signaling pathways. Int J Mol Sci 2021; 22: 8388.
54. Dong T, Zhao D, Jiang S, Gu Y, Wang C, Yang Q, *et al.* Kurarinone protects against renal injury and fibrosis after unilateral ureteral obstruction through enhancement of the Nrf-2 signaling pathway. J Mol Histol 2025; 56: 286.
55. Long L, Luo H, Wang Y, Gu J, Xiong J, Tang X, *et al.* Kurarinone, a flavonoid from Radix Sophorae Flavescentis, inhibits RANKL-induced osteoclastogenesis in mouse bone marrow-derived monocyte/macrophages. Naunyn Schmiedebergs Arch Pharmacol 2024; 397: 7071-7087.
56. Xiong Z, Yang H. Unraveling the pharmacological intricacies of kurarinone in osteoporosis: Insights from a network pharmacology approach. Pharmacog Mag 2024; 20: 1350-1358.
57. Xu X, Dong Q, Zhong Q, Xiu W, Chen Q, Wang J, *et al.* The flavonoid kurarinone regulates macrophage functions via aryl hydrocarbon receptor and alleviates intestinal inflammation in irritable bowel syndrome. J Inflamm Res 2021; 14: 4347-4359.
58. Pan Y, Deng B, Wang T, Zhou Z, Wang J, Gao C, *et al.* Kurarinone ameliorates intestinal mucosal inflammation via regulating T cell immunity. Front Immunol 2025; 16: 1587479.
59. Li Z, Lin M, Li Y, Shao J, Huang R, Qiu Y, *et al.* Total flavonoids of *Sophora flavescens* and kurarinone ameliorated ulcerative colitis by regulating Th17/Treg cell homeostasis. J Ethnopharmacol 2022; 297: 115500.
60. Li W, Li Y, Qiu Y, Huang R, Niu J, Chen J, *et al.* Kurarinone and Nor-kurarinone inhibit NLRP3 inflammasome activation and regulate macrophage polarization against ulcerative colitis. Int Immunopharmacol 2025; 157: 114758.
61. Gu C, Liu Y, Lv J, Zhang C, Huang Z, Jiang Q, *et al.* Kurarinone regulates Th17/Treg balance and ameliorates autoimmune uveitis via Rac1 inhibition. J Adv Res 2025; 69: 381-398.
62. Kim BH, Na KM, Oh I, Song IH, Lee YS, Shin J, *et al.* Kurarinone regulates immune responses through regulation of the JAK/STAT and TCR-mediated signaling pathways. Biochem Pharmacol 2013; 85: 1134-1144.
63. Ha NM, Son NT. Health benefits of fraxetin: From chemistry to medicine. Arch Pharm 2024; 357: e2400092.
64. Thoa NT, Son NT. Scutellarein: A review of chemistry and pharmacology. J Pharm Pharmacol 2025; 77: 352-370.
65. Ni HTN, Linh NN, Nhung PTT, Dao PTB, Manh VQ, Son NT. Icariside II: Natural occurrence, biotransformation, pharmacological activity, synthetic modification, pharmacokinetics, and bioavailability. J Pharm Pharmacol 2025; 77: 1491-1512.
66. Prete M, Dammacco R, Fatone MC, Racanelli V. Autoimmune uveitis: Clinical, pathogenetic, and therapeutic features. Clin Exp Med 2016; 16: 125-136.
67. YuQing G, GuoGuang S. Changes of peripheral blood T lymphocyte subsets and serum cytokine levels in patients with chronic hepatitis B receiving lamivudine and kurorinone treatment. J Clin Hepatol 2013; 16: 229-231.
68. He X, Zhang M, Yang Z, Ji R, Gong D, Li Y, *et al.* Natural parkin modulators drive mitophagy and overcome metabolic dysfunction-associated fatty liver disease. Ind Crop Prod 2025; 233: 121404.
69. Huang Y, Lin H, Chen Y, Huang X. Pharmacokinetic and bioavailability study of kurarinone in dog plasma by UHPLC-MS/MS. Biomed Chromatogr 2020; 34: e4945.
70. Yang Z, Zhang W, Li X, Shan B, Liu J, Deng W. Determination of sophoraflavanone G and kurarinone in rat plasma by UHPLC-MS/MS and its application to a pharmacokinetic study. J Sep Sci 2016; 39: 4344-4353.
71. Liu Y, Mo ZX, Wang CG, Huang R, Wang F, Chen L. Identification of metabolites of kurarinone from *Sophora flavescens* Ait in rat urine by ultra-performance liquid chromatography with linear ion trap orbitrap mass spectrometry. Trop J Pharm Res 2016; 15: 1299-1305.
72. Zhang X, Jiang P, Chen P, Cheng N. Metabolism of kurarinone by human liver microsomes and its effect on cytotoxicity. Pharm Biol 2016; 54: 619-627.
73. Qin Y, Zhu Y, Xue X, Zhou G, Li H, Wang J. An *in vitro* study for evaluating permeability and metabolism of kurarinone. Evid Based Complement Alternat Med 2020; 2020: 5267684.
74. Jiang P, Zhang X, Huang Y, Cheng N, Ma Y. Hepatotoxicity induced by *Sophora flavescens* and hepatic accumulation of kurarinone, a major hepatotoxic constituent of *Sophora flavescens* in rats. Molecules 2017; 22; 1809.